České Vysoké Učení Technické v Praze
Fakulta Strojní

Czech Technical University in Prague
Faculty of Mechanical Engineering

RNDr. Matej Daniel, Ph.D.

Mechanobiologie v diagnostice, terapii a rehabilitaci

Mechanobiology in diagnosis, therapy and rehabilitation

Summary

Degeneration of articular cartilage affects hundreds of millions of patients throughout the world. The onset of osteoarthritis and the progression of disease rest with a multiplicity of physical and biological factors. It is acknowledged, that the long term overloading eventually induces cartilage loss. Mechanobiology, a new scientific discipline, studies relationship between the long-term mechanical loading of biological tissue and tissue development and remodelling.

This lecture is focused on the application of mechanobiological analysis of the joint in the clinical practice in order to describe the status of the joint and to make appropriate intervention. Hip joint was chosen as an object of research as it is one of the most loaded joints in the human body. A mathematical model was developed which assess patient-specific loading based on standard anteroposterior radiogram.

Three stages of possible application of mechanobiological analysis are discussed: diagnosis, therapy and rehabilitation. Hips subjected to dysplasia, aseptic necrosis of the femoral head and hips after intraarticular acetabular fracture are considered mostly. Evidence-based analysis of cartilage mechanobiology in patient care is presented.

Souhrn

Degenerace kloubní chrupavky (artróza kloubu) je jednou z nejrozšířenějších nemocí vyššího věku. I když je vznik artrózy kloubu podmíněn velkým počtem biologických a fyzikálních faktorů, ukazuje se, že na vznik artrózy má velký vliv dlouhotrvající nadměrné zatížení kloubu. Vztahem mezi dlouhodobým mechanickým zatížením a vývojem a přestavbou biologické tkáně se zabývá nový vědní obor mechanobiologie.

Tato přednáška je zaměřena na využití metod mechanobiologické analýzy kloubu v klinické praxi pro popis stavu kloubu a aktivní ovlivnění tohoto stavu. Jako objekt výzkumu byl zvolen kyčelní kloub, protože se jedná o jeden z nejvíce zatěžovaných kloubů v lidském těle. Byl vyvinut model, který pro daného pacienta umožňuje stanovení individuálního zatížení kloubu na základě jeho RTG snímku.

Jsou diskutována tři stadia aplikace mechanobiologického modelu: stadium diagnozy, stadium terapie a stadium rehabilitace. Důraz je kladen hlavně na klouby postižené dysplázií, aseptickou nekrosou hlavice femuru a klouby s frakturou kloubní jamky. Na příkladech je ukázána přímá aplikace mechanobiologické analýzy v jednotlivých stádiích péče o pacienta.

Keywords : contact pressure; arthrosis; mathematical modelling

Klíčová slova : kontaktní tlak; artróza; matematické modelování

Contents

1 Introduction

1.1 What is mechanobiology

In a seminal paper defining mechanobiology as a new science discipline [18], van der Meulen and Huiskes wrote, that skeletal mechanobiology aims to discover "*how mechanical forces modulate morphological and structural fitness of the skeletal tissue – bone, cartilage, ligament, and tendon*". Mechanobiology in comparison with biomechanics moves the emphasis from mechanics to biology. Mechanobiology aims to establish predictive models of how mechanical forces cause changes in tissue phenotype, microstructure, and shape.

1.2 Articular cartilage mechanobiology

In diarthroidal joints, articular cartilage is able to distributes loads that reach up to seven times body weight as a result of specialized matrix macromolecules that provide compressive resistance and tensile strength. This aspect of tissue functionality is due to the three matrix constituents: water, aggrecans and type II collagen [9].Cartilage exhibits a certain hierarchical structure (Fig. 1).

Decades of research on cartilage have attempted to assess its mechanical, biochemical, physiological and pathophysiological mechanisms [17]. However, an accurate understanding of cartilage mechanobiology remains elusive. In mechanobiology of the cartilage, two principal tasks arises [3]:

1. define the mechanisms that cause the transformation from cartilage to bone tissue during skeletal growth and mechanisms that keeps articular cartilage at the end of long bones where it is needed for smooth movement

2. identify mechanisms that yield to cartilage degeneration in elderly in order to stop or postpone degeneration process.

2 Modelling cartilage mechanics

To describe mechanical properties of cartilage, an appropriate relationships between the stress and the strain should be identified in constitutive equations. Development of mathematical models of cartilage reflect gained information about cartilage structure and function (Fig. 1).

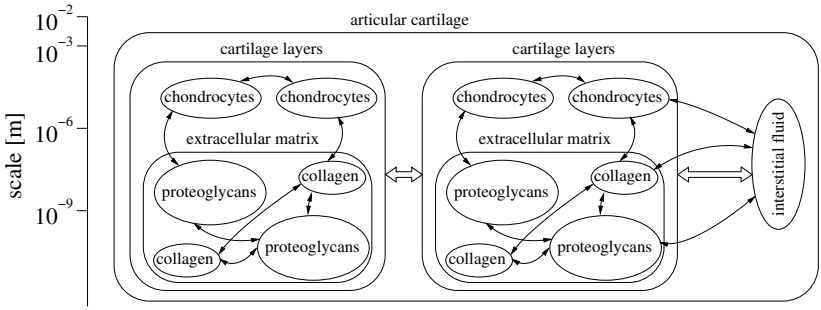

Figure 1: Cartilage structure: nano-scale molecules of glycoaminoglycan and collagen form micro-scale extracellular matrix with chondrocytes, the various zonal properties of which define the macro-scale cartilage layers. The whole articular cartilage is formed in the supra-scale (organ-scale) as a part of the whole joint.

It has been shown experimentally that for all cartilages, a remarkably linear relationship between the compressive stress and strain exists at equilibrium up to approximately 20% strain. Therefore, the **linear elastic model** was used to predict deformation of the cartilage in normal motion and the behavior of the cartilage was described using a Hooke's law.

It is generally accepted that for a more accurate description of the mechanical behavior of articular cartilage a **biphasic model** should be used. According to the biphasic theory [14] the tissue is assumed to consist of a compressible porous matrix, which consists of an compressible solid, hydrated with an incompressible fluid.

The total stress in the tissue is given by the sum of the solid and fluid stress

$$\sigma_{\text{tot}} = \sigma_E - p\mathbf{I} \tag{1}$$

where σ_E is the effective stress tensor, p is the hydrostatic fluid pressure and $\mathbf{I}$ the unit tensor. In the most biphasic models of the cartilage, the solid matrix is assumed linear elastic and isotropic and the effective stress tensor is given by

$$\sigma_E = \lambda e_s \mathbf{I} + 2\mu\epsilon \tag{2}$$

where e_s is the cubic dilatation, ϵ is the strain tensor, μ and λ are Lamé's constants.

In the absence of mass exchange, the total mass change must equal to the amount of fluid flow through the surface of the tissue. Hence,

the law of mass conservation is given by

$$\nabla \cdot \mathbf{v}_s + \nabla \cdot (n_f(\mathbf{v}_f - \mathbf{v}_s)) = 0 \tag{3}$$

where n_f is the fluid fraction and $\mathbf{v}_s$, $\mathbf{v}_f$ are the velocities of the solid and fluid phase, respectively. According to the Darcy's law, the fluid flow is related to the hydrostatic pressure.

$$n_f(\mathbf{v}_f - \mathbf{v}_s) = k\nabla p \tag{4}$$

where k is the hydraulic permeability. Using Eq. (4) in Eq. (3), it can be obtained:

$$\nabla \cdot \mathbf{v}_s + \nabla \cdot (k\nabla p) = 0 \tag{5}$$

The poroelastic model of the cartilage can be further extended to include orthotropy of the cartilage, different properties of collagen fibers in tension and in compression, fibril reinforcement or flow dependent viscoelasticity.

To describe a charged nature of macromolecules in a cartilage inducing cartilage swelling, a theory for a tertiary mixture – **triphasic mixture model** – has been developed, including the two fluid-solid phases (biphasic), and an ion phase, representing cations and anions, to describe the deformation and stress fields for cartilage under chemical and/or mechanical loads. Triphasic theory combines the physicochemical theory for ionic and polyionic (proteoglycan) solutions with the biphasic theory for cartilage.

The total stress is the same as for the biphasic model (Eq. (1)), but in this case the hydrostatic pressure is given by

$$p = \mu^f + \Delta\Pi \tag{6}$$

where μ^f is the electrochemical potential and $\Delta\Pi$ is the osmotic pressure gradient. In the absence of mass exchange the law of conservation of mass is given by

$$\frac{\partial}{\partial t} n_\alpha + \nabla \cdot (n_\alpha(v_\alpha - v_s)) = 0 \tag{7}$$

where n_α and v_α are volume fraction and velocity of component α, respectively. The relation between permeability and ion diffusion-convection, the velocity of component is described by Huyghe et al, 2002

$$-c_\beta \nabla \mu^\beta = \sum_{\alpha=f,+,-} \mathbf{B}_{\alpha\beta}(v_\alpha - v_s) \qquad \beta = f,+,- \tag{8}$$

where c_β is the molecular concentration of phase β per unit of mixture volume, μ^β its molecular potential and $\mathbf{B}$ a symmetric matrix of frictional coefficients. The osmotic pressure gradient from Eq. (6) is given by

$$\Delta\Pi = \Pi - \Pi_{\text{ext}} \tag{9}$$

where internal (Π) and external (Π_{ext}) osmotic pressures are given as

$$\Pi = \phi_{\text{in}} RT(c^+ + c^-) \tag{10}$$

$$\Pi_{\text{ext}} = \phi_{\text{in}} RT(c^+_{\text{ext}} + c^-_{\text{ext}}) \tag{11}$$

where R is the gas constant, T is the absolute temperature, c^+ and c^- are the concentrations of mobile cations and anions, respectively, ϕ_{in} and ϕ_{ext} are the internal and the external osmotic coefficients, respectively. At each point electroneutrality must hold, hence

$$c^+ = c^- + c_F \tag{12}$$

where c_F is the fixed charge density.

3 Clinical mechanobiology

The response of the articular cartilage on the mechanical loading can be studied at various level of cartilage hierarchical structure: from the study of subcellular structures to whole body study (Fig. 1) [2]. Within our studies, a hip joint was chosen as a model object. Hip joint is one the main weight-bearing joints in the human body and diseases of the hip joint yield to immobility of the patient.

To test the hypothesis, that mechanical loading considerably influence hip joint development in clinical studies, several mathematical models have been constructed [1]. The models used for retrospective studies should meet following criteria:

1. use data from archives (no additional examination of the patient is required)
2. model can be easily adjusted for individual patient
3. model should estimate loading force as well as distributed load on the articular cartilage

Considering limitations and availability of CT and NMR scans, a standard anteroposterior radiogram was taken as a basis for biomechanical model of hip loading within our model [11]. The model used in

our studies consists of two parts. First part is a model for estimation the hip joint force while the second is a model for evaluation the hip joint contact stress distribution.

3.1 Joint reaction force

Most of the previous studies use a one-legged stance as the most appropriate body position to evaluate hip joint loading. Hence, the one-legged stance was taken as basis also in our model if the motion history of the patient was unknown. However, in the one-legged stance, there is more muscles than needed to maintain equilibrium from the mechanical point of view – the problem being referred as the **muscle redundancy**. In our model, the musculoskeletal geometry defining positions of proximal and distal muscle attachment points in neutral position and cross-sectional areas ($PCSA$) of the muscles is based on the work of Delp et al., 1990 and on the work of Dostal & Andrews, 1981. We used a straight-line muscle model without taking into account the properties of the muscle-tendon unit. Muscle force required to maintain equilibrium F_i in a given position of body is computed using the method of inverse dynamic optimization proposed by Crowninshield et al., 1981.

$$\begin{aligned} \text{minimize} \quad & G(\mathbf{F}) = \sum_i \left(\tfrac{F_i}{PCSA_i} \right)^3 \\ \text{subject to} \quad & \mathbf{g}(\mathbf{F}) = \mathbf{0} \\ & \mathbf{l}_F \leq \mathbf{F} \leq \mathbf{u}_F \end{aligned} \tag{13}$$

where $g(\mathbf{F})$ are the equilibrium equations and $\mathbf{l}_F$ and $\mathbf{u}_F$ are the lower and the upper physiological constrains, respectively. The linearly constrained optimization problem was solved using a combination of linear programming and sequential quadratic programming using Broyden-Fletcher-Goldfarb-Shanno's technique.

3.2 Joint contact stress

For calculation of the contact stress distribution we have adapted three-dimensional mathematical model [11]. The model has been upgraded by utilizing discrete element analysis (DEA) method. The input parameters of the model [11] are the hip joint resultant force $\mathbf{R}$ and the geometry of the acetabulum (Fig. 2).

Within the model, it is assumed that femoral head bears again acetabulum separated by a cartilage layer (Fig. 2a) and the stress is proportional to the cartilage deformation in compression and shear. Cartilage

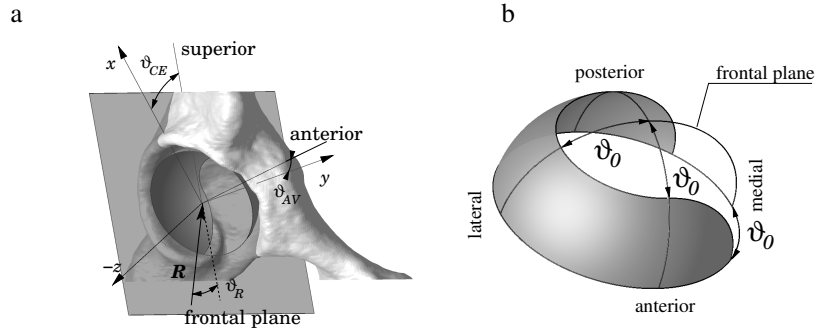

Figure 2: (a) Position of the acetabulum and direction of the loading force $\mathbf{R}$, ϑ_{CE} denotes the center-edge angle of Wiberg, ϑ_{AV} is the angle of anteversion and ϑ_R defines inclination of the hip joint force in the frontal plane. (b) Geometric model of the acetabular cartilage, ϑ_0 is the size of acetabular fossa.

surfaces are modeled as a series of normal and shear springs. The compressive and shear force in each spring element will be determined by the change of relative distance of the spring element attachment points in reference to the neutral or unloaded position. If a discrete element or rigid body moves by an external load, displacement of an arbitrary point on the rigid body can be expressed by vector $\mathbf{u}$:

$$\mathbf{u} = \mathbf{u}_G + \mathbf{q} \times (\mathbf{r} - \mathbf{r}_G) \tag{14}$$

where $\mathbf{u}_G$ is displacement vector of centroid and $\mathbf{q}$ is infinite small rotation vector and $(\mathbf{r} - \mathbf{r}_G)$ is the position vector of an arbitrary point with respect to a local coordinate fixed at the centroid G.

The relative displacement δ of contact point $\mathbf{r}$ on the boundary surface of two elements 1 and 2 was expressed as a function of the displacement of the centroid of two rigid bodies.

$$\delta = \mathbf{u}_2 - \mathbf{u}_1 = [\mathbf{B}]u \tag{15}$$

where

$$u^T = [u_1, v_1, w_1, \theta_1, \phi_1, \chi_i, u_2, v_2, w_2, \theta_2, \phi_2, \chi_2] \tag{16}$$

$$\delta^T = [\delta_x, \delta_y, \delta_z] \tag{17}$$

and the transformation matrix $[\mathbf{B}]$ was defined by Genda et al, 2001. The normal displacement δ_d and the tangential displacement δ_s of the

contact surface plane are given as follows:

$$\delta_d = \mathbf{n} \cdot \delta \tag{18}$$
$$\delta_s^2 = |\mathbf{n} \times \delta|^2 \tag{19}$$

where $n = [l, m, n]$ is the normal vector of each spring element on joint contact surface. The strain energy due to the relative displacement δ_d and δ_s of the spring elements distributed over the contact surface A can be given by following equation:

$$U = \frac{1}{2} \iint_A \left(k_d \delta_d^2 + k_s \delta_s^2 \right) \mathrm{d}A \tag{20}$$

where k_d is the normal spring stiffness and k_s is the shear spring stiffness. The strain energy can be derived as follows:

$$U = \frac{1}{2} \iint_A \left(\delta^T [\mathbf{D}] \delta \right) \mathrm{d}A \tag{21}$$

where

$$[\mathbf{D}] = \begin{bmatrix} k_d l^2 + k_s(1 - l^2) & (k_d - k_s)lm & (k_d - k_s)ln \\ (k_d - k_s)lm & k_d m^2 + k_s(1 - m^2) & (k_d - k_s)mn \\ (k_d - k_s)ln & (k_d - k_s)mn & k_d n^2 + k_s(1 - n^2) \end{bmatrix} \tag{22}$$

Using Eq. (15), the strain energy can be reduced to:

$$U = \frac{1}{2} u^T [\mathbf{K}] u \tag{23}$$

where

$$[\mathbf{K}] = \iint_A [\mathbf{B}]^T [D] [\mathbf{B}] \mathrm{d}A \tag{24}$$

Applying Castigliano's theorem to Eq. (23), the following equilibrium equation can be defined

$$\mathbf{R} = \frac{\partial U}{\partial u} = [\mathbf{K}] u \tag{25}$$

where $\mathbf{R}$ is generalized force vector. It is important to note that such analysis can only be applied under small displacement so that the strain energy of the system can be expressed in homogeneous quadratic function in order to apply the Castigliano's theorem. After calculation

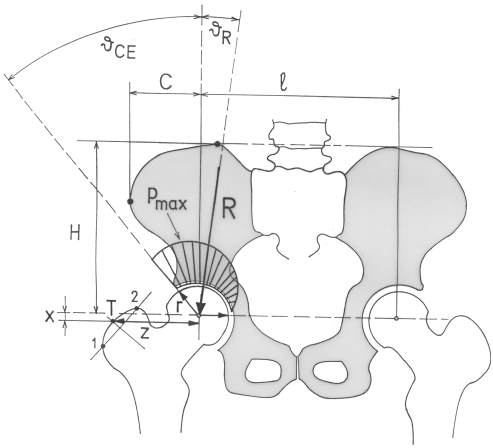

Figure 3: Characteristic parameters of the pelvis and proximal femur used to adjust model for calculation of the hip joint reaction force and contact stress distribution.

of the relative displacement u between the two rigid bodies, the strain of each normal and shear spring can be calculated using (15) and (18). The normal and shear force can be derived as follows:

$$p = \sigma = k_s \delta_s; \qquad \tau = k_d \delta_d \tag{26}$$

The spring stiffness property can be estimated from the contact surface material's elastic properties. Based on a liner elastic theory for a homogeneous and isotropic material, the spring constants could be derived as:

$$k_d = \frac{E(1-\nu)}{(1+v)(1-2v)h}; \qquad k_d = \frac{G}{h} \tag{27}$$

where E and G are the Young's modulus and the shear modulus, respectively and h is the cartilage thickness.

As the synovial joints are well lubricated only compressive, radial stresses (p) are further assumed. From the assumption of spherical bone surfaces of femur and hemispehrical acetabulum and analytical solution can be derived as:

$$\delta_s = \delta_{s0} \cos\gamma \tag{28}$$

where γ is the angle between the stress pole and any point at the articular surface and δ_{s0} is the cartilage deformation at the stress pole.

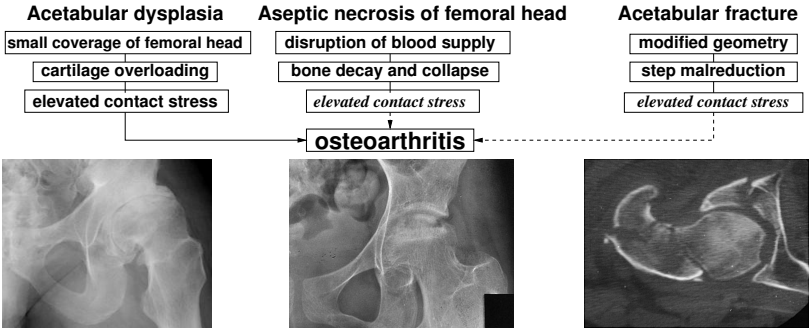

Figure 4: Loading induced oastarthritis is well accepted hypothesis for dysplastic hips. The relationship between the excessive hip loading and ostearthritis in hip subjected to aseptic necrosis of the femoral head and hip after the acetabular fracture is not straightforward.

3.3 Adaptation for individual patient

Particularities of the individual patient are taken into account by the characteristic geometry of the pelvis and the proximal femur and by the patient's body weight (W_B [N]).

The model for determining the force $\mathbf{R}$ in a one-legged stance takes into account patient-scaled muscle geometry [11]. The coordinates of muscle attachments are adjusted to each patient according to the geometry of the pelvis and the proximal femur (Fig. 3a).

To determine the stress distribution in a normal hip joint we must know the hip joint reaction force and additional geometrical parameters (Fig. 3b).

4 Diagnosis – identification of primary mechanism of cartilage degeneration

It is widely acknowledged that long-term elevated contact stress in dysplastic hips is responsible for cartilage degeneration in relatively youth patients. However, similarly rapid onset of osteoarthritis was observed also in hips subjected to aseptic necrosis of the femoral head and in hips with misaligned intraarticular fracture. It is interesting to determine level of the stress in these three diagnosis and to test whether the stress in dysplastic hips, hips after aseptic necrosis and hips with intraarticular fracture reaches the same level.

4.1 Study on dysplastic hips

Deviations in the size, shape, mutual proportions or orientation of the acetabulum and femoral head are described as hip dysplasia. The aims were to examine if the peak stress in dysplastic hips is higher than in normal hips and to find out which biomechanical parameter may be used to describe dysplasia in addition to morphological parameters.

Introducing polar coordinate system in acetabular coordinates, position of the stress pole (Θ_a) in dysplastic hips can be computed from

$$\tan(\vartheta_{Ra} + \Theta_a) = \frac{\sin^2 \Theta_a}{\pi - \Theta_a + \sin \Theta_a \cos \Theta_a} \tag{29}$$

where ϑ_{Ra} is the inclination of the hip joint force in acetabular coordinate system. The value of the stress at the pole is then determined from the expression:

$$p_0 = \frac{3\,R\,\cos(\vartheta_{Ra} + \Theta_a)}{2\,r^2\,(\pi - \Theta_a + \sin \Theta_a \cos \Theta_a)} \tag{30}$$

4.1.1 Stress level in dysplastic hips

By using a mathematical model of the adult human hip in the static one-legged stance position of the body (section 3), the forces acting on the hip, peak stress in the hip joint and other relevant radiographic and biomechanical parameters were assessed in clinical study. The average peak stress normalized to the body weight in dysplastic hips was markedly higher than the average normalized peak stress in normal hips (Tab. 1) [13].

4.1.2 Parameter describing mechanobiological status of the hip

In our study, the peak contact stress (p_{max}) and stress gradient index (G_p) are introduced for the assessment of dysplasia in human hip joint. The absolute value of G_p is equal to the magnitude of the gradient of

Hip	Count	p_{max}/Wb [kPa/N]
Normal	36	3.5
Dysplastic	47	7.1

Table 1: Clinical study of stress in normal and dysplastic hips.

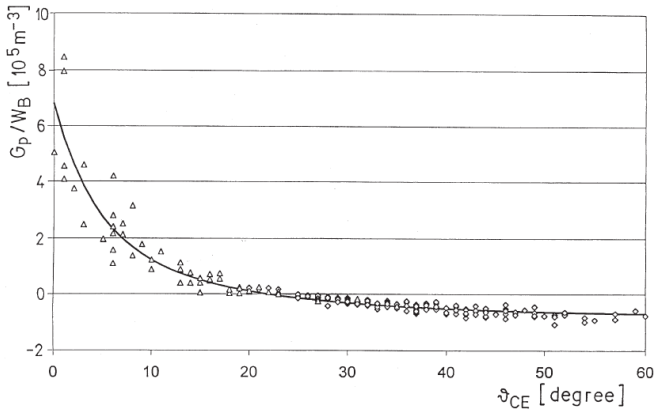

Figure 5: The correlation between the index of the stress gradient index (G_p) normalized with respect to the body weight (W_B) and the centre-edge angle ϑ_{CE}. The values for the normal hips are denoted by the symbol $\diamond$ and the values for the dysplastic hips are denoted $\triangle$.

Hip	Count	G_p/W_B [10^5 m^{-3}]
Normal	146	-0.445
Dysplastic	56	+1.481

Table 2: Gradient of contact stress in normal and dysplastic hips.

the contact stress at the lateral acetabular rim.

$$G_p = \left| \frac{\partial p}{\partial r}\mathbf{e}_r + \frac{1}{r}\frac{\partial p}{\partial \vartheta}\mathbf{e}_\vartheta + \frac{1}{r\sin\vartheta}\frac{\partial p}{\partial \varphi}\mathbf{e}_\varphi \right| = -\frac{p_0}{r}\sin(\vartheta_{CE} - \Theta) \qquad (31)$$

where $\mathbf{e}_r$, $\mathbf{e}_\vartheta$ and $\mathbf{e}_\varphi$ are the orthogonal spherical unit vectors, Θ is position of the stress pole and stress distribution is given by Eqs. (26) and (28) [16].

The average value of G_p/W_B changes its sign at the value of the center-edge angle $\vartheta_{CE} = 20^\circ$ which is usually considered as the boundary value of ϑ_{CE} (lower limit) for the normal hips. Accordingly we suggest a new definition for the hip dysplasia with respect to the size and sign of the normalized stress gradient index G_p/W_B. The hips with positive G_p/W_B are considered to be dysplastic while the hips with negative G_p/W_B are considered to be normal.

4.1.3 Mechanobiological parameters and functional status of dysplastic hip

In the clinical practice the patient's subjective feeling of pain and the patient's mobility are often considered to be more important than the outcome of the biomechanical analysis of the hip. Therefore, the relationship between the Harris hip score, stress gradient index and peak contact stress was tested. Statistically significant correlation between the G_p/W_B, p_{max} and Harris Hip Score was found. Hips were divided into two normal and dysplastic group according to G_p and ϑ_{CE} (Tab. 3).

Criterion	Normal (Count)	Dysplastic (Count)	Difference
sign G_p	$G_p < 0$ (16)	$G_p > 0$ (29)	$p < 0.05$
size ϑ_{CE}	$\vartheta_{CE} < 20°$ (10)	$\vartheta_{CE} > 20°$ (35)	$p = 0.233$

Table 3: Evidence-based determination of hip dysplasia and clinical status. Statistical difference was evaluated by Kolmogorov-Smirnov test.

4.2 Contact stress in hips subjected to aseptic necrosis of the femoral head

Avascular necrosis (osteonecrosis) is characterized by a decay of the bone tissue due to disruption of the blood supply to the diseased region of the bone [4]. As a result, mechanical properties of the bone change so that its ability to bear load is reduced with respect to the healthy hip. Secondary to osteonecrosis, the hip is likely to develop osteoarthritis.

We present evidence supporting the hypothesis that osteoarthritis in hips with aseptic necrosis of the femoral head can be caused by elevated contact stress related to the reduced load-bearing ability of the necrotic bone.As the estimated values of stress in hips with osteonecrosis are in the range obtained by the same method in dysplastic hips, osteoarthritis in hips with osteonecrosis can be caused by elevated contact stress.

4.3 Contact stress after incongruent reduction of acetabular fracture

Posttraumatic arthrosis is the most common complication of intraarticular acetabular fracture. Clinical and experimental studies clearly show, that the incidence of posttraumatic arthrosis is greater in patient with persistent displacement of fracture fragment.

Type	AW	AC	PW	PC	TT	JT	IT
p_{max} [MPa] Offset	4.64	4.94	3.79	4.99	4.96	1.53	1.56
p_{max} [MPa] Stepoff	3.71	3.42	3.64	3.44	3.00	4.37	3.77

Table 4: Stress after malreduction of acetabular fracture according to fracture type. AW anterior wall, AC anterior column, PW posterior wall, PC posterior column, TT transtectal, JT juxtatectectal, IT infratectal. Stress in normal hip $p_{max} = 1.56$ MPa.

We have developed a model which calculates a stress distribution after malreduced acetabular fracture. If the fracture line passes superior acetabular region, peak contact stress is considerably increased and reaches the values observed in dysplastic hips (section 4.1). The results confirm a hypothesis that increased stress within the hip joint eventually leads to arthrosis.

5 Mechanobiologically supported therapy

It was shown in the previous section, that increased contact stress is a common parameter which may be responsible for cartilage degeneration in various diseases. One of the major goals in managing these joints is the prevention or postpone of arthrosis. Therapy can in principle be either surgical (osteotomies, open reduction, total hip replacement) or conservative (closed reduction, drug therapy).

Our model can be used in clinical practice as to assess the risk that the elevated stress poses upon the development of coxarthrosis. High stress indicates that the surgical intervention is favorable while low stress indicates that the decision for the operation can be postponed, regarding the risk for coxarthrosis development.

5.1 Osteotomies - alternative to total hip arthroplasty

In prevention of ostearthritis, the goal of osteotomy is to restore anatomy to as normal state as possible and thereby to eliminate excessive load to the joint caused by the abnormal joint mechanics. In our work we have studied two types of ostotomies:

Salter osteotomy - it was shown, that unfavorable stress distribution induces development of dysplasia over time [19].

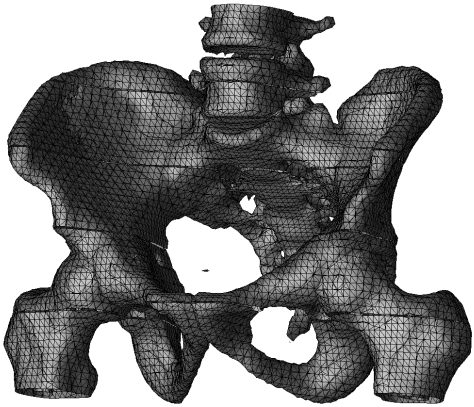

Figure 6: Geometry of proximal pelvis and acetabulum obtained from CT images for given patient by method suggested by Daniel et al, 2005. Following geometry can by used in DEA method to calculate contact stress distribution.

Intertrochanteric osteotomy - our results support the hypothesis that the hips with a more favorable postoperative distribution of contact hip stress have a better clinical outcome [7].

6 Design of appropriate rehabilitation

In the joint treated by conservative therapy, an appropriate rehabilitation scheme should be suggested in order to prevent long term elevated stress acting upon cartilage. Also in the hip treated surgically, appropriate therapy should be designed so, that the operated segments will not be overloaded.

6.1 Therapy after acetabular fractures

Operative fixation of fragments in acetabular fracture treatment is not strong enough to allow weight bearing before the bone is healed. In some patients, even passive or active nonweight-bearing exercises could lead to dislocation of fragments and posttraumatic osteoarthritis. Therefore, early rehabilitation should avoid loading the acetabulum in the regions of fracture lines. The aim of our work is to estimate acetabular loading in nonweight-bearing upright, supine, and side-lying leg abduction (Tab. 5). Spatial distribution of the average acetabular loading

Abduction	supine	supine supported	side-lying	upright
p_{max}	1.3 MPa	0.2 MPa	1.2 MPa	0.5 MPa

Table 5: Peak stresses during rehabilitation abduction

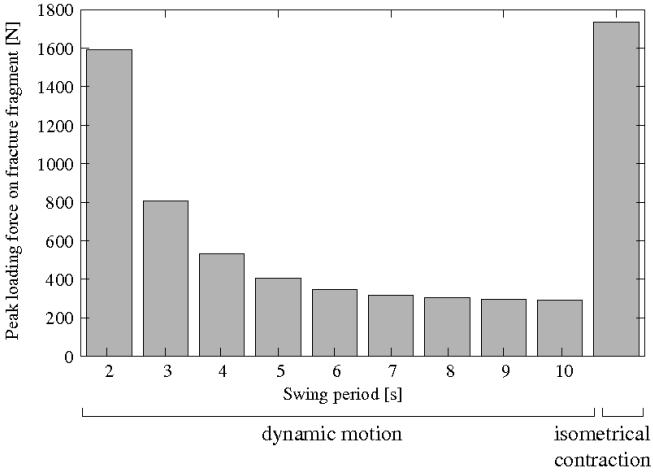

Figure 7: Peak force acting on the acetabular fracture fragment in dynamic supine unsupported abduction with range 0°-40° for various swing period τ and in maximum isometrical contraction.

shows that early rehabilitation should be planned according to location of the fracture lines [12].

6.2 Reducing fast motion in early rehabilitation

In a case study, patient after anterior column fracture was treated by closed reduction through Kocher-Langenbeck approach. Very fast abduction motion around the operated hip caused dislocation of bony fragments. Mathematical simulation shows that fast motion may load the operated fracture fragment up to 1.8 kN.

6.3 Managing occupational activities

It was shown recently that the incidence of coxarthrosis is higher in patients frequently walking upstairs. We have shown that the stress in walking downstairs may be for 115% higher than in normal walking.

The increased incidence of arthrosis in patients who frequently walk upstairs is actually the consequence of their walking downstairs (which normally follows previously walking upstairs). .

7 Conclusions

The data from mathematical modelling and retrospective clinical studies presented within this lecture leads to following:

Mechanobiological analysis is a suitable tool in identification the cause of disease, suggestion of appropriate therapy and design of individual rehabilitation plan.

The most significant questions in cartilage mechanobiology that should further be solved includes application of whole joint mechanobiology at the cell level. Such research will have a direct impact in the field of functional tissue engineering. Further studies should include also the mechanobiology of the bone in addition to mechanobiology of the cartilage.

Further study of the cartilage mechanobiology will contribute to three important long term goals.

1. Development of new techniques of cartilage replacement in tissue engineering.

2. Computer-assisted design of surgical procedures that could forestall the need for total hip arthroplasty based on understanding the precise role of mechanical loading on cartilage repair.

3. Development of new classes of drugs to prevent progression of osteoarthritis utilizing the knowledge on the cell level.

References

[1] Brand, R. (2005). Joint contact stresses: A reasonable surrogate for biological processes? *The Iowa Orthopaedic Journal*, 25:82–94.

[2] Buckwalter, J. A. and Mankin, H. J. (1998). Articular cartilage: tissue design and chondrocyte-matrix interactions. *Instr Course Lect*, 47:477–486.

[3] Carter, D. R., Wong, M., and Orr, T. E. (1991). Musculoskeletal ontogeny, phylogeny, and functional adaptation. *J Biomech*, 24 Suppl 1:3–16.

[4] Daniel, M., Herman, S., Dolinar, D., Iglic, A., Sochor, M., and Kralj-Iglic, V. (2006). Contact stress in hips with osteonecrosis of the femoral head. *Clin Orthop Relat Res*, 447:92–99.

[5] Daniel, M., Iglic, A., and Kralj-Iglic, V. (2008). Hip contact stress during normal and staircase walking: the influence of acetabular anteversion angle and lateral coverage of the acetabulum. *J Appl Biomech*, 24(1):88–93.

[6] Daniel, M., Iglič, A., and Kralj-Iglič, V. (2005). The shape of acetabular cartilage optimizes hip contact stress distribution. *Journal of Anatomy*, 207:85–91.

[7] Dolinar, D., Antolic, V., Herman, S., Iglic, A., Kralj-Iglic, V., and Pavlovcic, V. (2003). Influence of contact hip stress on the outcome of surgical treatment of hips affected by avascular necrosis. *Arch Orthop Trauma Surg*, 123(10):509–513.

[8] Genda, E., Iwasaki, N., Li, G., MacWiliams, B., Barrance, P., and Chao, E. (2001). Normal hip joint contact pressure distribution in single-leg standing – effect of gender and anatomic parameters. *Journal of Biomechanics*, 34:895–905.

[9] Huber, M., Trattnig, S., and Lintner, F. (2000). Anatomy, biochemistry, and physiology of articular cartilage. *Invest Radiol*, 35(10):573–580.

[10] Huyghe, J. M., Janssen, C. F., Donkelaar, C. C. V., and Lanir, Y. (2002). Measuring principles of frictional coefficients in cartilaginous tissues and its substitutes. *Biorheology*, 39(1-2):47–53.

[11] Iglič, A., Kralj-Iglič, V., Daniel, M., and Maček-Lebar, A. (2002). Computer determination of contact stress distribution and the size of the weight-bearing area in the human hip joint. *Computer Methods in Biomechanics and Biomedical Engineering*, 5:185–192.

[12] Kristan, A., Mavcic, B., Cimerman, M., Iglis, A., Tonin, M., Slivnik, T., Kralj-Iglic, V., and Daniel, M. (2007). Acetabular loading in active abduction. *IEEE Trans Neural Syst Rehabil Eng*, 15(2):252–257.

[13] Mavčič, B., Pompe, B., Daniel, M., Iglič, A., and Kralj-Iglič, V. (2002). Mathematical estimation of stress distribution in normal and dysplastic human hip. *Journal of Orthopaedic Research*, 20:1025–1030.

[14] Mow, V., C.S., P., and Kelly, M. (1999). Biomechanics of articular cartilage. In Nordin, M. and Frankel, V., editors, *Basic biomechanics of the musculoskeletal system*, pages 31–58. Lea & Febiger, London.

[15] Mow, V. C., Ratcliffe, A., and Poole, A. R. (1992). Cartilage and diarthrodial joints as paradigms for hierarchical materials and structures. *Biomaterials*, 13(2):67–97.

[16] Pompe, B., Daniel, M., Sochor, M., Vengust, R., Kralj-Iglič, V., and Iglič, A. (2003). Gradient of contact stress in normal and dysplastic human hip. *Medical Engineering & Physics*, 25:379–385.

[17] Smith, R. L. (2008). Mechanical loading effects on articular cartilage matrix metabolism and osteoarthritis. In Joseph A. Buckwalter, Martin Lotz, S. J.-F., editor, *Osteoarthritis, inflammation and degeneration: A continuum*, pages 14–30. IOS Press.

[18] van der Meulen, M. C. H. and Huiskes, R. (2002). Why mechanobiology? a survey article. *J Biomech*, 35(4):401–414.

[19] Vengust, R., Daniel, M., Antolič, V., Zupanc, O., Iglič, A., and Kralj-Iglič, V. (2001). Biomechanical evaluation of the hip after innominate osteotomy: a long-term follow-up study. *Archives of Orthopaedic and Trauma Surgery*, 121:511–516.

RNDr. Matej DANIEL, Ph.D.

Education

2004	**Ph.D.** Biomechanics	Faculty of Mechanical Engineering Czech Technical University in Prague Czech Republic
2002	**RNDr.** Biophysics & Molecular Physics	Faculty of Mathematics, Physics and Informatics Comenius University, Slovakia
2001	**M.Sc.** Biomedical Physics	Faculty of Mathematics, Physics and Informatics Comenius University, Slovakia

Research Experience

2006–	**Senior Researcher**	Faculty of Mechanical Engineering Czech Technical University in Prague
2006	**Senior Researcher**	Faculty of Electrical Engineering University of Ljubljana
2004-2006	**Research Assistant**	Faculty of Mechanical Engineering Technical University of Košice
2002-2004	**Junior Researcher**	Faculty of Mechanical Engineering Czech Technical University in Prague

Teaching Experience

2009–	**Nanobiomechanics**	lecture
2007–	**Biomechanical laboratories**	seminar
2002–	**Strength of Materials**	seminar
2007–2008	**Biophysics**	lecture
2004-2006	**Statics**	seminar
2004-2006	**Mechanics**	seminar

Awards

2006	SICOT Poster Award, Buenos Aires
2005	Werner von Siemens Excellence Award, Prague
2005	Zvoníček Foundation Award, Prague
2004	Prize of Prof. Valenta and Prof. Čihák, Prague

Professional Interest and Expertise

Clinical Biomechanics; Nanobiomechanics; Mechanobiology